Inorganic Chemistry

Article

pubs.acs.org/IC

Molecular Vibration Spectroscopy Studies on Novel Trinuclear Rhodium-7-Hydride Complexes of the General Type $\{[Rh(PP^*)X]_3(\mu_2\text{-}X)_3(\mu_3\text{-}X)\}(BF_4)_2$ (X = H, D)

Christina Kohrt,[†] Sven Hansen,[†] Hans-Joachim Drexler,[†] Uwe Rosenthal,[†] Axel Schulz,*[,‡] and Detlef Heller*[,†]

[†]Leibniz-Institut für Katalyse e.V. an der Universität Rostock, Albert-Einstein-Straße 29a, 18059, Rostock, Germany

[‡]Universität Rostock, Institut für Chemie, Albert-Einstein-Straße 3a, 18059 Rostock, Germany

Supporting Information

ABSTRACT: Novel trinuclear rhodium-hydride complexes with diphosphine ligands Tangphos, *t*-Bu-BisP*, and Me-DuPHOS which contain bridging μ_2- and μ_3-hydrides as well as terminal hydrides in one molecule have been reported recently. In this work, these different rhodium-hydride bonds are characterized by Raman spectroscopy and the results are compared with those obtained by means of the more commonly applied IR spectroscopy. Density functional theory (DFT) calculations have been carried out to support the experimental findings. The structure of the Rh_3H_7 core is described in the context of their vibrational stretching modes.

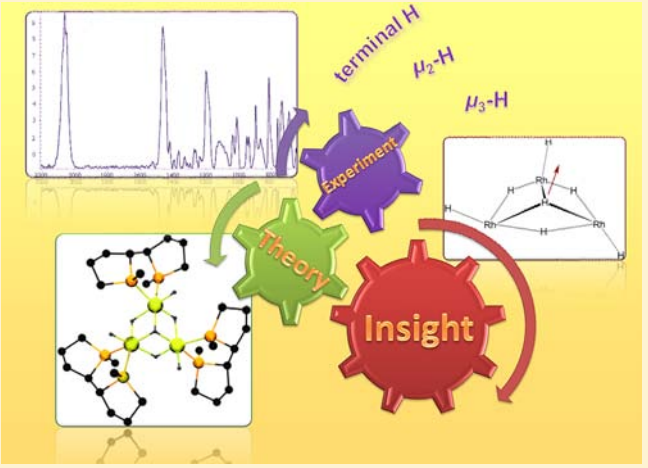

INTRODUCTION

Transition metal hydrides play a central role in many homogeneous catalytic reactions.[1] Especially Rhodium-hydrides are very important in hydrogenation or hydroformylation reactions.[2,3] The characterization of hydrides is commonly carried out by NMR spectroscopy, X-ray analysis or neutron diffraction.[4] Alternatively, rhodium-hydrides are characterized by IR spectroscopy.

Already in 1965, Wilkinson et al. described a Rh−H vibration of about 2000 cm^{-1} for a Rh-phosphine-hydride complex.[5] In a review from 1972 all hitherto known IR data of terminal rhodium-hydrides (ν(Rh−H)) with monodentate phosphine ligands were summarized and discussed.[6] More recent research on the IR spectroscopic characterization of rhodium-phosphine complexes (including chelating phosphines) is summarized in ref 7. The length of the Rh−H bond, which is influenced by the steric and electronic properties of the ancillary ligands, determines the IR (vibrational) frequency. For terminal hydrides ν(Rh−H)-values between 1930 cm^{-1} and 2260 cm^{-1} are expected.[7]

Literature data on the IR spectroscopic characterization of the Rh-hydride vibration of Rhodium complexes which contain μ_2- or μ_3-bridging hydrides (μ_2: edge bridging) are scarce.[7f,8] Evidently a broadening of bands is characteristic. IR frequencies around 1650 cm^{-1} have been described for μ_2-bridging hydrides ν(Rh−H···Rh).[7f,8a]

To the best of our knowledge no literature data are available on the Raman spectroscopic characterization of Rh hydrides, although the relevance of such a technique for the detection especially of bridging metal-hydride bonds has already been pointed out in ref 6 ["Raman spectroscopy will prove to be of great help in discerning bridging metal−hydrogen modes too weak and broad to be seen in the infrared"].

Recently, we reported on the synthesis and characterization of novel trinuclear rhodium complexes with chiral diphosphine ligands Tangphos, *t*-Bu-BisP*, and Me-DuPHOS (Scheme 1).[9]

Scheme 1. Chiral Diphosphine Ligands

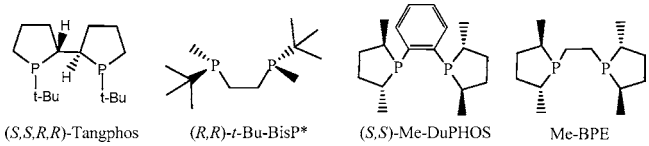

The compounds were fully characterized by X-ray analysis (in case of the Tangphos complex all hydrides could be

Received: April 19, 2012
Published: June 21, 2012

   dx.doi.org/10.1021/ic300802d | *Inorg. Chem.* 2012, 51, 7377−7383

determined from the electron density), NMR, ESI-MS, as well as IR spectroscopy.

Since such complexes contain bridging μ_2- and μ_3-hydrides as well as terminal hydrides in one molecule, they can serve as model compounds for systematic investigations by means of vibrational spectroscopy. In this work, Raman spectroscopy has been applied for the first time to characterize different rhodium-hydride bonds. The results have been compared to those obtained from conventional IR spectroscopy. Density functional theory (DFT) calculations were carried out to manifest the correct structure (distances and angles) of the C_3 symmetric Rh_3H_7 core in these novel trinuclear rhodium complexes and to allow assignment of the different Rh−H stretching modes.

RESULTS AND DISCUSSION

Besides the already characterized trinuclear rhodium-hydride complexes with ligands Tangphos, *t*-Bu-Bis-P*, and Me-DuPHOS, a similar complex with the Me-BPE ligand[10] could be synthesized for the first time. The trinuclear Rh−H complex was characterized by X-ray analysis, NMR spectroscopy, and electrospray ionization-mass spectrometry (ESI-MS). The molecular structure of $\{[Rh(Me\text{-}BPE)H]_3(\mu_2\text{-}H)_3(\mu_3\text{-}H)\}(BF_4)_2$ is shown in Figure 1.

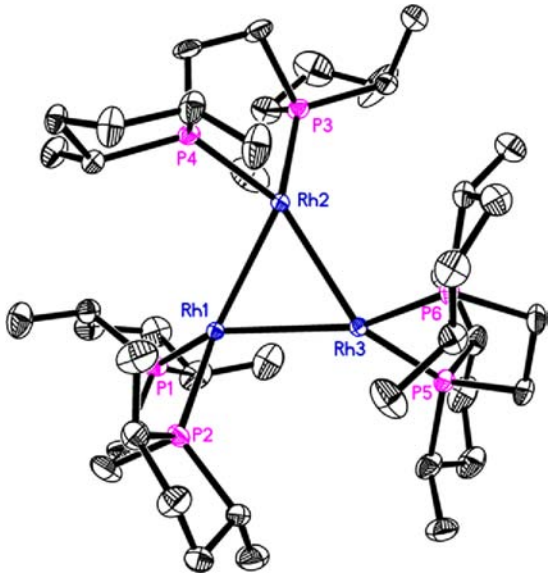

Figure 1. Molecular structure of the cation in the trinuclear Me-BPE rhodium-hydride complex (ORTEP, 30% probability ellipsoids). Hydrogen atoms (of the ligand) were omitted for clarity. The three rhodium atoms are disordered over two positions with occupancies of 0.92 to 0.08. The rhodium atoms with the major occupancy (92%) are shown. Selected distances [Å] and angles [deg]: Rh−Rh 2.744−2.768(2), Rh−P 2.214−2.298(2); P−Rh−P 84.66−85.63(6).[11]

Unfortunately, also in this case (in analogy to the complexes with ligands *t*-Bu-BisP* and Me-DuPHOS[9]) the hydrogen atoms could not be refined from the electron density. However, the hydride region of the ^{1}H NMR spectrum (Figure 2) shows the expected seven hydrides in an intensity ratio of 3:1:3.

$\{[Rh(Me\text{-}BPE)H]_3(\mu_2\text{-}H)_3(\mu_3\text{-}H)\}(BF_4)_2$ crystallizes from methanol as orange crystals in the monoclinic space group $P2_1$ with one disordered MeOH molecule per unit cell. The determined structural parameters are in good agreement with those of $\{[Rh(Tangphos)H]_3(\mu_2\text{-}H)_3(\mu_3\text{-}H)\}(BF_4)_2$.[9] Since hydrogen atoms cannot be exactly located by means of single

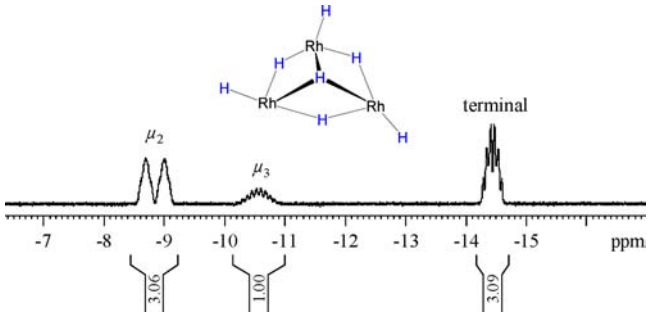

Figure 2. ^{1}H NMR spectrum (hydride region) of the isolated crystals of the trinuclear hydride complex $\{[Rh(Me\text{-}BPE)H]_3(\mu_2\text{-}H)_3(\mu_3\text{-}H)\}(BF_4)_2$ in CD_2Cl_2 (−8.8 ppm, −10.5 ppm, and −14.4 ppm). On the top is the Rh_3H_7 framework.

crystal X-ray analysis, the exact structure of the $P_6Rh_3H_7$ framework is still unknown (see below).

Exploratory measurements had already shown that all these complexes were both Raman and IR active in the hydride region, thereby Raman spectroscopy is easier to perform under anaerobic conditions. To verify and to aid the assignment of the bands measured by IR and Raman spectroscopy the complex $\{[Rh(Tangphos)H]_3(\mu_2\text{-}H)_3(\mu_3\text{-}H)\}(BF_4)_2$[12] was subjected to DFT calculations. To reduce computational costs, the diphosphine ligand was slightly simplified by replacing the ^{t}Bu groups by Me groups ($\{[Rh(\text{“}Me\text{-}Tangphos\text{”})H]_3(\mu_2\text{-}H)_3(\mu_3\text{-}H)\}(BF_4)_2$).

The hybrid functional B3LYP[13,14] along with the all electron triple-ζ basis set SVP[15] was employed to optimize the geometry and to calculate the Hessian matrix to obtain the vibrational frequencies. The Gaussian09 Rev. A.02[16] program suite was used. The optimization was performed in C_3 symmetry.[17]

The optimized structure of the $P_6Rh_3H_7$ framework (Figure 3) displays a strongly distorted octahedral environment for

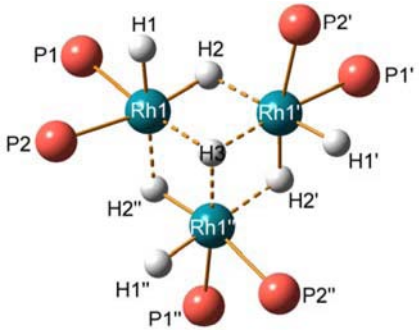

Figure 3. Calculated C_3 symmetric $P_6Rh_3H_7$ framework in $(\{[Rh(\text{“}Me\text{-}Tangphos\text{”})H]_3(\mu_2\text{-}H)_3(\mu_3\text{-}H)\}(BF_4)_2)$, selected distances in Å, angles in deg: Rh1−H1 1.557, Rh1−H2 1.703, Rh1−H3 1.939, Rh1−H2″ 1.919; H1−Rh1−H2 85.4, H1−Rh1−H3 99.5, H1−Rh1−H2″ 178.8, H1−Rh1−P1 80.0, H1−Rh1−P2 85.1, H2−Rh1−H3 85.5, H2−Rh1−H2″ 95.7, H3−Rh1−H2″ 79.92325, Rh1−H2−Rh1′−H2′ 82.4, H2−Rh1′−H2′−Rh1″ −77.5.

each Rh atom with four significantly different Rh−H bond lengths (Rh1−H1 1.557, Rh1−H2 1.703, Rh1−H3 1.939, Rh1−H2″ 1.919 Å, cf. $\sum r_{cov}$(Rh−H) 1.57 and $\sum r_{vdW}$(Rh−H) = 3.0 Å).[18,19] As expected the shortest bond is found for the terminal hydrogen atoms (H1), while for the bridging H2 atom two considerably different distances are computed (Rh1−H2 1.703 vs Rh1−H2″ 1.919 Å) indicating the existence of three

dx.doi.org/10.1021/ic300802d | Inorg. Chem. 2012, 51, 7377−7383

Table 1. Calculated Vibrational Frequencies (cm^{-1}) for the Three Different Rhodium-*Hydride* Bonds in {[Rh("Me-Tangphos")H]$_3$(μ_2-H)$_3$(μ_3-H)}(BF$_4$)$_2$ in Comparison with Experimental Data of {[Rh(Tangphos)H]$_3$(μ_2-H)$_3$(μ_3-H)}(BF$_4$)$_2$

approximately assign. to H bond[a]		Γ	$\tilde{\nu}_{calc}$ (I_{IR}/I_{Raman})[b]	$\tilde{\nu}_{exp,\ Raman}$ (I_{Raman})[c]	$\tilde{\nu}_{exp,IR}$ (I_{IR})
terminal-H	$\nu_{1,2}$	E	2062 (166/89)	*d*	2061 (vw,br)
	ν_3	A	2060 (24/899)	2061 (10,br)	*d*
μ_2-H	$\nu_{4,5}$	E	1502 (747/14)	1523 (0.02)	1518 (w,br)
	ν_6	A	1490 (47/148)	1463 (9,br)	*e*
	$\nu_{7,8}$	E	1102 (286/115)	1115 (2,br)	1110 (m,sh)[e,f]
	ν_9	A	1066 (10/237)	1078 (2,br)[f]	*e*
μ_3-H	ν_{10}	A	1150 (2/296)	1120 (2,br)	1110 (m,sh)[e,f]

[a]Approximate form of selected normal modes is depicted in Figure 3. [b]IR intensities in km mol^{-1} and Raman activities in $Å^4\ u^{-1}$ in brackets (I_{IR}/I_{Raman}), [c]scaled intensities (0−10); [d]hidden in the unresolved broad peak of $\nu_{1/2}$ or ν_3; [e]superimposed by vibrations of the backbone; [f]tentative assignment.

Table 2. Calculated Vibrational Frequencies (cm^{-1}) for the Three Different Rhodium-*Deuteride* Bonds in {[Rh("Me-Tangphos")D]$_3$(μ_2-D)$_3$(μ_3-D)}(BF$_4$)$_2$ in Comparison with Experimental Data of {[Rh(Tangphos)D]$_3$(μ_2-D)$_3$(μ_3-D)}(BF$_4$)$_2$

approximately assign. to D bond[a]		Γ	$\tilde{\nu}_{calc}$ (I_{IR}/I_{Raman})[b]	$\tilde{\nu}_{exp,\ Raman}$ (I_{Raman})[c]	$\tilde{\nu}_{exp,IR}$ (I_{IR})
terminal-D	$\nu_{1,2}$	E	1466 (63/32)	*d*	1460 (m,sh)
	ν_3	A	1465 (1/174)	1474 (10,br)	*d*
μ_2-D	$\nu_{4,5}$	E	1067 (298,7)	*e*	1025 (s,sh)
	ν_6	A	1057 (23,72)	1068 (1,br)	*e*
	$\nu_{7,8}$	E	779 (273/72)	n.o.	788 (m,sh)[f]
	ν_9	A	757 (12/134)	718 (2,sh)	712 (w,sh)
μ_3-D	ν_{10}	A	815 (1,138)	805 (5,br)[f,g]	788 (w,sh)[f,g]

[a]Approximate form of selected normal modes is depicted in Figure 3. [b]IR intensities in km mol^{-1} and Raman activities in $Å^4\ u^{-1}$ in brackets (I_{IR}/I_{Raman}). [c]Scaled intensities (0−10). [d]Hidden in the unresolved broad peak of $\nu_{1/2}$ or ν_3. [e]Hidden in the unresolved broad peak of $\nu_{4/5}$ or ν_6. [f]Superimposed by vibrations of the backbone. [g]This peak is also found for the H species but is much broader and asymmetric in the spectra of the D species.

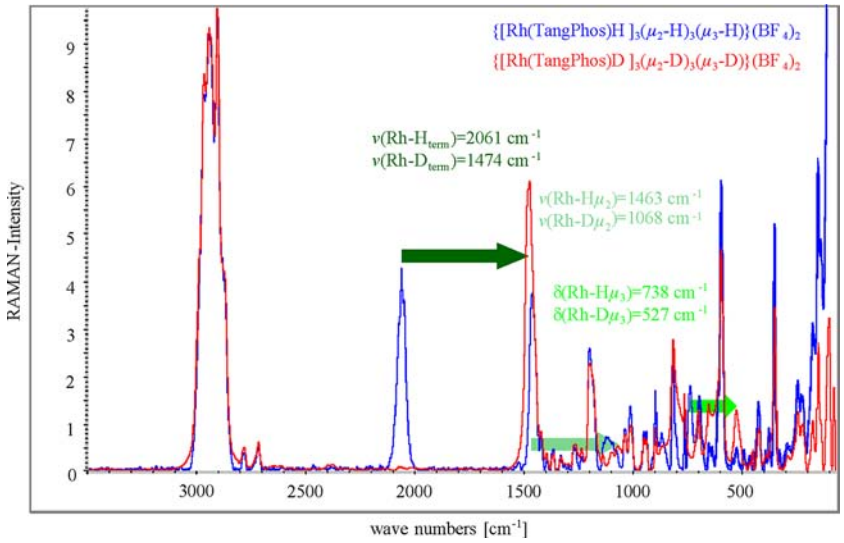

Figure 4. Raman spectra of the trinuclear 7 Hydride- (blue) {[Rh(Tangphos)H]$_3$(μ_2-H)$_3$(μ_3-H)}(BF$_4$)$_2$ and 7 Deuteride-TangPhos-Rhodium complex {[Rh(Tangphos)D]$_3$(μ_2-D)$_3$(μ_3-D)}(BF$_4$)$_2$ (red). The isotopic shift is illustrated by the green arrows. The shift from 738 to 527 cm^{-1} is an isotopic shift of the strongly Raman active deformation mode.

strongly asymmetric Rh−H···Rh hydrogen bonds. The central corrugated six-membered Rh_3H_3 ring (Rh1−H2−Rh1′−H2′ 82.4) adopts a chair conformation, and is capped by one μ_3 coordinating hydrogen atom (that is part of the C_3 axis), thus forming the main structural motif of such rhodium−hydrogen cluster complexes. In accord with C_3 symmetry, all three μ_3-H3−Rh distances are equally long with 1.939 Å.

Comparison of the computed data for the gas phase species with experimental data obtained from single crystal structure elucidation (vide supra) exhibit differences for the non hydrogen atoms in bond lengths no larger than 0.05 Å and in bond angles <0.6°. For instance the calculated Rh···Rh distance of 2.811 Å compares well with 2.771−2.789(1) Å determined by single crystal X-ray analysis.[9]

It was of interest to study the different Rh−H vibrational modes associated with the different Rh−H bonds. Moreover, to study isotopic shifts and to support the assignment in the experimentally observed data, also a frequency analysis was carried out for the deuterated species. A complete list of all hydrogen involving vibrations together with the approximate

dx.doi.org/10.1021/ic300802d | Inorg. Chem. 2012, 51, 7377−7383

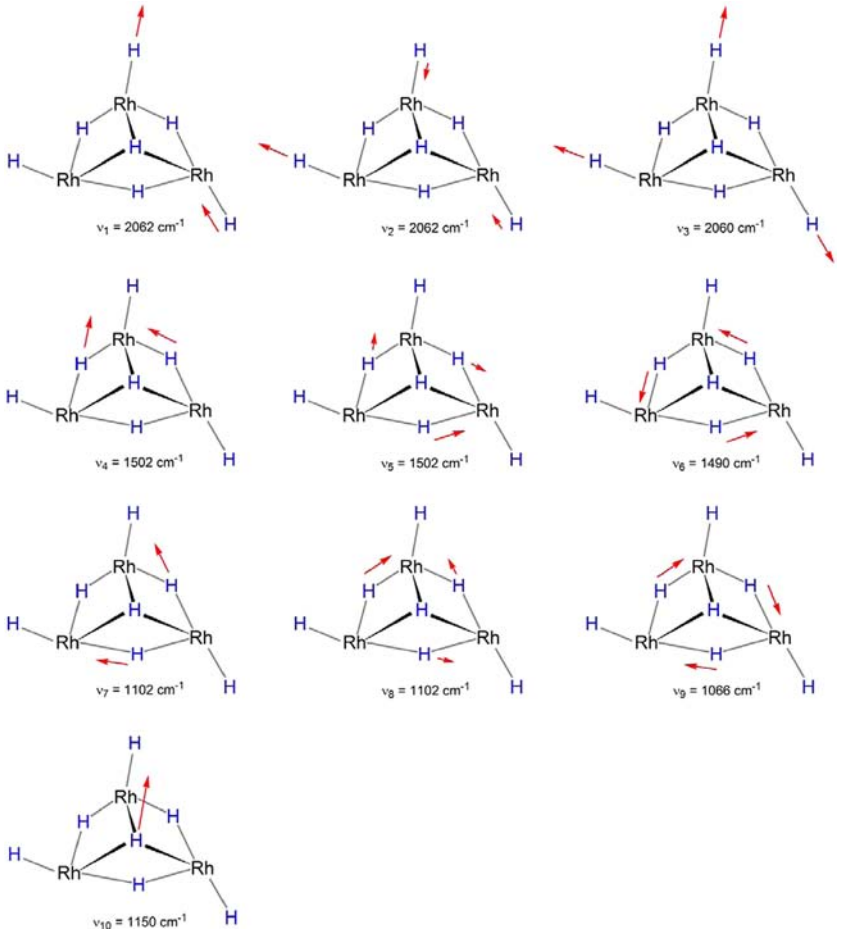

Figure 5. Approximate form of selected normal modes of $\{[Rh(\text{“Me-Tangphos”})H]_3(\mu_2\text{-}H)_3(\mu_3\text{-}H)\}(BF_4)_2$ (only Rh_3H_7 unit shown for clarity) describing Rh−H stretching vibrations.

assignment can be found in the Supporting Information. The calculated wave numbers of normal modes describing Rh−X stretching vibrations in the Rh−X framework (X = H, D) of model compound $\{[Rh(\text{“Me-Tangphos”})X]_3(\mu_2\text{-}X)_3(\mu_3\text{-}X)\}(BF_4)_2$ are summarized in Tables 1 and 2 along with approximate assignments. It should be noted that, although the harmonic approximation was used and the *t*-Bu group was substituted by a methyl group in the computation, the experimental vibrational data of $\{[Rh(Tangphos)X]_3(\mu_2\text{-}X)_3(\mu_3\text{-}X)\}(BF_4)_2$ agree well with the theoretically obtained data of $\{[Rh(\text{“Me-Tangphos”})X]_3(\mu_2\text{-}X)_3(\mu_3\text{-}X)\}(BF_4)_2$ (maximal deviation less than 40 cm^{-1}, average deviation 17 cm^{-1}). This might be attributed mainly to the fact that the light hydrogen atoms move in a fairly rigid (heavy atom) Rh-triangle, and the ligand backbone with the substituted methyl groups has no big influence on the hydrogen/deuterium normal modes within the Rh_3X_7 framework. As depicted in Figure 5, ten characteristic normal modes were identified describing dominantly Rh−X stretching vibrations (X = H). For X = D similar normal modes are found but at lower wave numbers (cf. Tables 1 and 2). Three vibrations can be assigned to the *terminal* hydrogen atoms (H1). While in ν_3 at 2060 cm^{-1} all H1 atoms vibrate in phase and this mode is strong in the Raman spectrum, the doubly degenerate modes $\nu_{1,2}$ at 2062 cm^{-1} describes a 180°-out-of-phase movement and are very weak in the IR spectrum. For the three μ_2-*bridged*-H−Rhodium bonds six different vibrational modes are observed. Because of the strong asymmetry along the Rh−H···Rh moieties (cf. Rh1−H2 1.703 vs Rh1···H2″ 1.919 Å, Figure 3) these two sets of three modes are found at significantly different wave numbers (1502/1490 vs 1102/1066 cm^{-1}). As discussed before, each set consists of an in-phase vibration, which is strong in the Raman but weak in the IR spectrum; and two out-of-phase vibrations, which are weak or absent in the Raman but strong in the IR spectrum. Vibrational mode ν_7 at 1150 cm^{-1} describes the μ_3-H−Rh bond stretch, which is strongly Raman active but very weak in the IR spectrum and slightly coupled with ν_3 (vice versa). As shown by experiment and theory, there is a significant shift upon H/D substitution decreasing the lower the wave numbers for the H species. Thus, the largest H/D shift is found for ν_1−ν_3 with about 600 cm^{-1}, followed by ν_4−ν_7 with about 435 cm^{-1} and ν_{10} with about 335 cm^{-1} in accord with experiment.

In agreement with theory, the *experimental* IR spectrum of $\{[Rh(Tangphos)H]_3(\mu_2\text{-}H)_3(\mu_3\text{-}H)\}(BF_4)_2$ (Supporting Information, Figure S4a) displays a weak band at 2061 cm^{-1} for the terminal Rh−H vibrations (cf. $\{[Rh(t\text{-}Bu\text{-}BisP^*)H]_3(\mu_2\text{-}H)_3(\mu_3\text{-}H)\}(BF_4)_2$: 2058 cm^{-1},[9] $\{[Rh(Me\text{-}BPE)H]_3(\mu_2\text{-}H)_3(\mu_3\text{-}H)\}(BF_4)_2$: 2043 cm^{-1}, Supporting Information, Figure S1) which is the strongest in the Raman spectrum (Table 1, Figure 4, Supporting Information, Figures S5−S6). To show that this band indeed corresponds to the terminal rhodium-hydride band, two similar complexes were synthesized and investigated: the deuterated analogue $\{[Rh(Tangphos)D]_3(\mu_2\text{-}$

dx.doi.org/10.1021/ic300802d | *Inorg. Chem.* 2012, 51, 7377−7383

D)$_3$(μ_3-D)}(BF$_4$)$_2$ and a trinuclear complex bearing no hydride at all, {[Rh$_3$(Tangphos)$_3$(μ_3-Cl)$_2$]BF$_4$. Indeed, the IR/Raman spectra of these hydride-free complexes do not show this band in the area of characteristic group frequencies around 2060 cm^{-1} (Supporting Information, Figures S4 b+c). However, for the deuterated complex {[Rh(Tangphos)D]$_3$(μ_2-D)$_3$(μ_3-D)}-(BF$_4$)$_2$ a new band appears at 1460 cm^{-1} (IR) and more obvious at 1474 cm^{-1} (Raman), respectively, which can be assigned to the terminal Rh−D vibrations (ν_{1-3}) based on the DFT-calculations (Tables 1−2, Figure 4, Supporting Information, Figures S7−S8). The deviation between experimental and computed wave numbers is less than 10 cm^{-1}.

In accordance with previously reported results,[8] the vibration of the μ_2-bridging hydrogen atoms of {[Rh(Tangphos)H]$_3$(μ_2-H)$_3$(μ_3-H)}(BF$_4$)$_2$ (ν_{4-6}, Figure 2, Table 1) can be assigned unequivocally to the experimentally observed band at 1463 cm^{-1} in the Raman spectrum (Supporting Information, Figure S8), which agrees well with the calculated bands at 1490 cm^{-1} and 1502 cm^{-1} (cf. {[Rh(*t*-Bu-BisP*)H]$_3$(μ_2-H)$_3$(μ_3-H)}-(BF$_4$)$_2$: 1460 cm^{-1} (Supporting Information, Figure S3), {[Rh(Me-BPE)H]$_3$(μ_2-H)$_3$(μ_3-H)}(BF$_4$)$_2$: 1448 cm^{-1} (Supporting Information, Figure S2). In the corresponding IR spectra the μ_2-bridging Rh−H vibrations (ν_{4-6}) can only tentatively be assigned and not unequivocally because of overlap with other vibrations of the backbone.

In the deuterated complex, the μ_2-Rh−D vibrations ν_{4-6} are found at 1068 cm^{-1} (Raman) and 1025 cm^{-1} (IR), respectively, displaying a strong H/D shift of 395 cm^{-1} (Raman) in accord with our calculations (Tables 1−2, Supporting Information, Figures S9−S10). Because of overlapping with other vibrations of the backbone, ν_{10} of the μ_3-bridging hydride can only be tentatively assigned to the wave numbers at 1120 cm^{-1} (Raman) and 1110 cm^{-1} (IR), respectively, and shifts to 805 cm^{-1} (Raman)/788 cm^{-1} (IR) in the deuterated species (Supporting Information, Figures S11−S12).

Besides the above-discussed Rh−X stretching vibrations, a strong Raman active deformation mode of the Rh$_3$H$_7$ core is found at 738 cm^{-1} (ν_{calc} = 713 (E) and 702 (A) cm^{-1}) which shifts to 527 cm^{-1} (ν_{calc} = 516 (E) and 506 (A) cm^{-1}) in the spectra of the D species (Figure 4). This strong H/D shift of 211 cm^{-1} is clearly visible in the fingerprint region of the Raman spectra, and it is characteristic for such trinuclear rhodium diphosphine complexes {[Rh(PP*)H]$_3$(μ_2-H)$_3$(μ_3-H)}(BF$_4$)$_2$ which contain terminal, μ_2-bridging, and μ_3-bridging hydrides between three rhodium atoms.

CONCLUSIONS

In summary, the structure of the P$_6$Rh$_3$X$_7$ (X = H, D) framework in cationic complexes of the type {[Rh(bidentate P-ligand)X]$_3$(μ_2-X)$_3$(μ_3-X)}$^{2+}$ was studied combining experiment and theory. The structure was found to have distorted octahedrally coordinated Rh centers connected by three asymmetric Rh−X···Rh hydrogen bonds with two distinctly different Rh−μ_2-X bond lengths. Thus, a strongly corrugated six-membered Rh$_3$H$_3$ ring with chair conformation is formed which is additionally capped by a μ_3-coordinating X atom maintaining the overall C_3 symmetry.

The vibrational frequencies of terminal-, μ_2-, and μ_3-bridging X$^-$ of the trinuclear rhodium-complexes {[Rh("Me-Tangphos")X]$_3$(μ_2-X)$_3$(μ_3-X)}(BF$_4$)$_2$ were calculated and experimentally determined by Raman and IR spectroscopy for the {[Rh(Tangphos)X]$_3$(μ_2-X)$_3$(μ_3-X)}(BF$_4$)$_2$ species. Inspection of the normal modes describing dominantly Rh−X stretching vibrations exhibits 10 different modes which are almost completely uncoupled and observed in well separated regions: (i) about 2060 cm^{-1} for the terminal Rh−X$_{terminal}$ bonds, (ii) about 1500 cm^{-1} for the bridging Rh−μ_2-X bonds, and (iii) 1150 cm^{-1} for tricoordinated Rh−μ_3-X bond. Interestingly, because of the strong asymmetry in the Rh−μ_2-X bonds along the Rh−X···Rh units, a second region is found at about 1050−1110 cm^{-1} displaying mainly the Rh···X bond vibration while the region around 1500 cm^{-1} is best described by the Rh−X stretching vibration.

The bands in the measured Raman/IR spectra were assigned by comparison with the analogous fully deuterated compound and with the computed frequencies. The hitherto commonly used IR spectroscopy for the characterization of terminal hydrides in rhodium complexes was shown to be less suitable than Raman spectroscopy because of the lower intensity especially for the Rh−H$_{terminal}$ stretching modes. The fact that Raman active frequency ν_3 lies in the range of characteristic group frequencies together with the pronounced H/D shift makes especially this normal mode a good indicator for a successful H/D exchange and proves the presence of a Rh$_3$H$_7$ framework in addition to NMR studies when X-ray analysis fails to locate the H atoms. For this reason Raman spectroscopy in combination with computations provides a powerful tool for the identification of complexes bearing a Rh$_3$H$_7$ core. It should be noted that besides ν_{1-3} all other frequencies are often superimposed by normal modes of the backbone or appear only as a shoulder. Only the close inspection of the H- and D-species Raman/IR spectra in combination with the computed frequencies allowed an approximate assignment.

EXPERIMENTAL SECTION

General Information. All manipulations were carried out under oxygen- and moisture-free conditions under argon using standard Schlenk or drybox techniques.

Diethyl ether was distilled from sodium benzophenone ketyl immediately prior to use. MeOH was freshly distilled from Magnesia turnings prior to use, CD$_3$OD from LiAlH$_4$ while CD$_2$Cl$_2$ were distilled from CaH$_2$. Subsequent removal of traces of oxygen for both deuterated solvents was carried out by application of six freeze−thaw cycles. (*R*,*R*)-Me-BPE (98%, Strem) and NaCl (99.5%, MERCK) were used as received. [Rh(PP*)(diolefine)]BF$_4$ complexes of the ligand Tangphos and Me-BPE were synthesized analogously to ref 20, and {[Rh(Tangphos)H]$_3$(μ_2-H)$_3$(μ_3-H)}(BF$_4$)$_2$ have been reported previously.[9]

NMR. ^{31}P{^{1}H}, ^{13}C{^{1}H}, ^{13}C DEPT, and ^{1}H NMR spectra were obtained on a Bruker ARX-300 or ARX-400 spectrometer at 297−298 K and were referenced internally to the deuterated solvent (^{13}C, CD$_2$Cl$_2$: $\delta_{reference}$ = 54 ppm, CD$_3$OD: $\delta_{reference}$ = 49.2 ppm) or to protic impurities in the deuterated solvent (^{1}H, CDHCl$_2$: $\delta_{reference}$ = 5.31 ppm, CD$_3$OD: $\delta_{reference}$ = 3.32 ppm). For chemical shifts in ^{31}P{^{1}H} NMR spectra, 85% H$_3$PO$_4$ was used as an external standard. The chemical shifts are given in ppm.

IR. Nicolet 6700 FT-IR spectrometer from BRUKER OPTIK GMBH with a Smart Endurance ATR device (ATR platinium diamond/ZnSe). The IR spectra were measured with a resolution of 2 cm^{-1}, replotted in absorbance, normalized to 100%, and baseline corrected (program OMNIC).

Raman. Bruker VERTEX 70 FT-IR with RAM II FT-Raman module, equipped with a Nd:YAG laser (1064 nm). Raman spectra were measured with a resolution of 1 cm^{-1} and a laser output of 200 mW and baseline corrected.

CHN Analyses. Leco CHNS-932 elemental analyzer.

Melting Points. E/Z-Melt, Standford Research Systems. Melting points are uncorrected and were measured in sealed capillaries.

dx.doi.org/10.1021/ic300802d | *Inorg. Chem.* 2012, 51, 7377−7383

MS (ESI-TOF). The mass spectrometric measurements were performed on a Time-of-Flight LC/MS 6210 (Agilent Technologies). Ionization was carried out by Electrospray ionization.

X-ray Structure Determination. Single crystals of complex $\{[Rh(Me\text{-}BPE)H]_3(\mu_2\text{-}H)_3(\mu_3\text{-}H)\}(BF_4)_2$ suitable for X-ray diffraction studies were obtained by recrystallization from methanol, selected and mounted in inert oil under nitrogen, and transferred to the cold gas stream of the diffractometer. The sample was cooled to 123(2) K during measurement. Diffraction data were collected on a STOE-IPDS II diffractometer using graphite monochromated Mo−Kα radiation. The structure were solved by direct methods (SHELXS-97)[21] and refined by full matrix least-squares techniques against F^2 (SHELXL-97).[21] XP (Siemens Analytical X-ray Instruments, Inc.) was used for structure representations. Numerical absorption corrections were applied (X-SHAPE, X-RED32).[22] The nonhydrogen atoms, except the atoms of the solvent (methanol), were refined anisotropically. The hydrogen atoms were placed into theoretical positions (except the hydrogen atoms of the solvent methanol) and were refined by using the riding model. The seven expected hydrides could not be determined from the electron density. The weighting scheme used in the last cycles of refinement are is $\omega = 1/[\sigma^2(F_o^2) + (0.000498P)^2 + 0.0000P]$.

$\{[Rh(Me\text{-}BPE)H]_3(\mu_2\text{-}H)_3(\mu_3\text{-}H)\}(BF_4)_2$. A red solution of [Rh(Me-BPE)(NBD)]BF_4 (0.1 mmol, 54 mg) in MeOH (1 mL) was hydrogenated for 5 h at room temperature. The resulting orange solution was layered with diethyl ether under hydrogen atmosphere. Orange crystals were obtained on the next day. The crystals were washed with diethyl ether. Isolated yield: 33 mg (79%). Mp: 145 °C (dec., under Ar). Anal. Calcd for $C_{42}H_{91}P_6B_2F_8P_6Rh_3$: C, 39.9; H, 7.25. Found: C, 40.01; H, 7.25. MS (ESI-TOF): calculated for M^{2+} ($C_{42}H_{91}P_6Rh_3$): 545.135; Found: 545.136. ^{1}H NMR ($CDHCl_2$): δ −14.4 (br. s, 3H), −10.5 (m, 1H), −8.8 (d, 3H, J_{P-H} = 91.6 Hz), 0.94 (dd, 9H, CH_3, J_{P-H} = 18.94 Hz, J_{H-H} = 7.1 Hz), 1.06 (dd, 9H, CH_3, J_{P-H} = 18.18 Hz, J_{H-H} = 6.9 Hz), 1.15−1.37 (br m, 24H [18H CH_3, 6H CH_2]), 1.4−1.77 (br m, 12H, CH), 1.8−2.35 (br m, 30 H, CH_2). ^{13}C NMR (CD_2Cl_2): δ 13.0 (CH_2), 14.3 (CH_2), 19.7 (CH_2), 20.7 (CH_2), 25.5 (br m, CH), 27.7 (br m, CH), 33.9 (CH_3), 35.5 (CH_3), 37.6 (CH_2), 37.9 (CH_2), 38.0 (CH_2), 38.25 (CH_2), 40.6 (CH_2), 40.9 (CH_2), 44.3 (CH_2), 44.8 (CH_2). $^{31}P\{^1H\}$ NMR (CD_2Cl_2): δ 117.1 (d, J_{P-Rh} = 119.7 Hz), 95.5 (d, J_{P-Rh} = 106.1 Hz). IR/Raman: data can be found in the main text.

$\{[Rh(Tangphos)D]_3(\mu_2\text{-}D)_3(\mu_3\text{-}D)\}(BF_4)_2$. The $\{[Rh(Tangphos)\text{-}D]_3(\mu_2\text{-}D)_3(\mu_3\text{-}D)\}(BF_4)_2$ complex was synthesized by our recently reported method (ref 9) with the exception that we used D_2 instead of H_2 and deuterated methanol CD_3OD instead of CH_3OH. The crystals were washed with diethyl ether. Isolated yield: 44%. Mp: 139 °C (dec., under Ar). Anal. Calcd for $C_{48}H_{96}D_7B_2F_8P_6Rh_3$: C, 42.53; H, 8.18. Found: C, 42.68; H, 7.86. MS (ESI-TOF): calculated for M^{2+} ($C_{48}H_{96}[2H]_7P_6Rh_3$): 590.7; Found: 590.703. ^{1}H NMR ($CDHCl_2$): δ 1.04 (d, 27H, *t*-Bu, J_{P-H} = 14.6 Hz), 1.15 (d, 27H, *t*-Bu, J_{P-H} = 15 Hz), 1.6−1.9 (br m, 12H, CH_2), 2.1−2.4 (br m, 12H, CH_2), 2.48−2.65 (br m, 12 H, CH_2), 2.65−2.9 (br m, 6H, CH). ^{13}C NMR (CD_2Cl_2): δ 25.7 (CH), 27.5 (CH_2), 28.4 (CH_3), 28.9 (CH_3), 29.2 (CH_2), 32.8 (C), 33.0 (C), 33.9 (CH_2), 34.1 (CH_2), 35.9 (CH_2), 36.8 (CH_2). $^{31}P\{^1H\}$ NMR (CD_2Cl_2): δ 133.9 (d, J_{P-Rh} = 110.2 Hz), 121.9 (d, J_{P-Rh} = 94.6 Hz). IR/Raman: data can be found in the main text.

$\{[Rh_3(Tangphos)_3(\mu_3\text{-}Cl)_2]BF_4$. This complex was obtained by hydrogenation of the [Rh(TangPhos)(COD)]BF_4 (0.08 mmol, 46.8 mg) complex in MeOH (1 mL) for 15 min and subsequent removal of hydrogen gas from the yellow solution by application of three freeze−thaw cycles. A solution of NaCl in MeOH was added to the frozen out solvate complex, and an orange precipitate could be isolated. Isolated yield: 9.7 mg (27%). Mp: 129 °C (dec., under Ar). MS (ESI-TOF): calculated for M^+ ($C_{48}H_{96}Cl_2P_6Rh_3$): 1237.247; Found: 1237.249. ^{1}H NMR (CD_3OD): δ 1.34 (d, 27H, *t*-Bu, J_{P-H} = 13.3 Hz), 1.55−2.04 (br m, 36H), 2.04−2.17 (br m, 6H). ^{13}C NMR (CD_3OD): δ 27.4 (CH_2), 29.1 (CH_2), 29.5 (CH_3), 34.8 (C), 37.1 (CH_2), 46.7 (CH). $^{31}P\{^1H\}$ NMR (CD_3OD): δ 120.5 (d, J_{P-Rh} = 200.9 Hz).

■ ASSOCIATED CONTENT

Ⓢ Supporting Information

Crystallographic data, details related to the DFT-calculation, and the experimental as well as the calculated Raman and IR spectra. This material is available free of charge via the Internet at http://pubs.acs.org.

■ AUTHOR INFORMATION

Corresponding Author

*E-mail: axel.schulz@uni-rostock.de (A.S.), detlef.heller@catalysis.de (D.H.). Phone: (+49)381 498-6400 (A.S.), (+49) 381-1281-183 (D.H.). Fax: (+49) 381-1281-51183 (D.H.).

Notes

The authors declare no competing financial interest.

■ ACKNOWLEDGMENTS

We thank Prof. X. Zhang and Chiralquest for providing the Tangphos ligand. We also thank DC C. Roth and Prof. R. Ludwig, University of Rostock, for the Raman measurements.

■ REFERENCES

(1) (a) Dedieu, A., Ed.; *Transition Metal Hydrides*; VCH Publishers, Inc.: New York, 1992. (b) Bau, R., Ed.; *Transition Metal Hydrides* , Adv. Chem. Ser. 167; American Chemical Society: Washington, DC, 1978.

(2) (a) deVries, H. G.; Elsevier, C. J., Eds.; *Handbook of Homogeneous Hydrogenation*; Wiley-VCH: Weinheim, Germany, 2007. (b) Gridnev, I. D.; Imamoto, T. *Acc. Chem. Res.* **2004**, *37*, 633−643. (c) Brown, J. M. *Chem. Soc. Rev.* **1993**, *22*, 25−41. (d) Landis, C. R.; Halpern, J. *J. Am. Chem. Soc.* **1987**, *109*, 1746−1754.

(3) vanLeeuwen, P.; Claver, C., Eds.; *Rhodium Catalyzed Hydroformylation*; Kluwer: Dordrecht, The Netherlands, 2000.

(4) To locate the hydride positions from electron density, crystals of very high quality are necessary. It should be noted that single crystal X-ray analysis is not suited for the *exact* experimental localization of hydrogen atoms. This is just possible through diffraction on the nucleus that is neutron diffraction. Crystal structure analysis by neutron diffraction requires bigger crystals than those suitable for X-ray analysis, and the method is less accessible.

(5) Young, J. F.; Osborn, J. A.; Jardine, F. H.; Wilkinson, G. *Chem. Commun.* **1965**, 131−132.

(6) Kaesz, H. D.; Saillant, R. B. *Chem. Rev.* **1972**, 231−281.

(7) (a) Ezhova, M. B.; Patrick, B. O.; Sereviratne, K. N.; James, B. R.; Waller, F. J.; Ford, M. E. *Inorg. Chem.* **2005**, *44*, 1482−1491. (b) Nishihara, Y.; Takemura, M.; Osakada, K. *Organometallics* **2002**, *21*, 825−831. (c) Iglesias, M.; Del Pino, C.; Nieto, J. L.; Garcia Blanco, S.; Martinez Carrera, S. *Inorg. Chim. Acta* **1988**, *145*, 91−98. (d) Fryzuk, M. D.; MacNeil, P. A.; Rettig, S. J. *J. Am. Chem. Soc.* **1987**, *109*, 2803−2812. (e) Iglesias, M.; Del Pino, C.; Nieto, J. L. *Inorg. Chim. Acta* **1986**, *119*, 7−12. (f) Bianchini, C.; Mealli, C. C.; Sabat, M. *J. Chem. Soc., Chem. Commun.* **1986**, 777−779. (g) Ott, J.; Venanzi, L. M.; Ghilardi, C. A.; Midollini, S.; Orlandini, A. *J. Organomet. Chem.* **1985**, *291*, 89−100. (h) Drago, R. S.; Miller, J. G.; Hoselton, M. A.; Farris, R. D.; Desmond, M. J. *J. Am. Chem. Soc.* **1983**, *105*, 444−449. (i) Tiethof, J. A.; Peterson, J. L.; Meek, D. W. *Inorg. Chem.* **1976**, *15*, 1365−1370. Data for similar rhodium hydrides that do not contain phosphines: (j) Yu, X.-Y.; Sun, H.; Patrick, B. O.; James, B. R. *Eur. J. Inorg. Chem.* **2009**, *13*, 1752−1758. (k) Li, C.; Widjaja, E.; Chew, W.; Garland, M. *Angew. Chem., Int. Ed.* **2002**, *41*, 3786−3789. (l) Bakac, A.; Thomas, L. M. *Inorg. Chem.* **1996**, *35*, 5880−5884. (m) Duckett, S. B.; Haddleton, D. M.; Jackson, S. A.; Perutz, R. N.; Poliakoff, M.; Upmacis, R. K. *Organometallics* **1988**, *7*, 1526−1532.

(8) (a) Albinati, A.; Eckert, J.; Hofmann, P.; Rüegger, H.; Venanzi, L. M. *Inorg. Chem.* **1993**, *32*, 2377−2390. (b) Woodcock, C.; Eisenberg,

R. *Inorg. Chem.* **1984**, *23*, 4207−4211. (c) Sutherland, B. R.; Cowie, M. *Inorg. Chem.* **1984**, *23*, 1290−1297.
(9) Fischer, C.; Kohrt, C.; Drexler, H.-J.; Baumann, W.; Heller, D. *Dalton Trans.* **2011**, *40*, 4162−4166.
(10) (a) Burk, M. J.; Feaster, J. E.; Harlow, R. L. *Tetrahydron: Asymmetry* **1991**, *2*, 569−592. (b) Burk, M. J.; Feaster, J. E.; Nugent, W. A.; Harlow, R. L. *J. Am. Chem. Soc.* **1993**, *115*, 10125−10138.
(11) Lines between the Rh atoms neither display bonds nor the correct connectivity since the bridging hydrogen atoms are missing.
(12) We choose Tangphos because it is the more interesting ligand for the planned catalytic reactions and because it was possible to refine all hydrides in the X-ray structure from their electron density.[9]
(13) Becke, A. D. *J. Chem. Phys.* **1993**, *98*, 5648−5652.
(14) Despite the fact that dispersion forces are not taken into account with B3LYP it is usually quite successful in predicting accurate molecular structure and vibrational frequencies (Scott, A. P.; Radom, L. *J. Phys. Chem.* **1996**, *100*, 16502). B3LYP hybrid functional was used for the sake of comparability, and frequency values are known to be corrected by an semiempirical factor [0.96 for B3LYP/6-31G(d)] which was not used here. In general it is to note, that frequency values for terminal hydrides are very reasonable while they are slightly overestimated for μ_2 bridged hydrides and overestimated for the μ_3 hydride. This is most likely due to the basis set which does not include diffuse functions but is a compromise between computational cost, as we have a quite large system, and accuracy..
(15) Schaefer, A.; Huber, C.; Ahlrichs, R. *J. Chem. Phys.* **1994**, *100*, 5829−5835.
(16) Frisch, M. J.; Trucks, G. W.; Schlegel, H. B.; Scuseria, G. E.; Robb, M. A.; Cheeseman, J. R.; Scalmani, G.; Barone, V.; Mennucci, B.; Petersson, G. A.; Nakatsuji, H.; Caricato, M.; Li, X.; Hratchian, H. P.; Izmaylov, A. F.; Bloino, J.; Zheng, G.; Sonnenberg, J. L.; Hada, M.; Ehara, M.; Toyota, K.; Fukuda, R.; Hasegawa, J.; Ishida, M.; Nakajima, T.; Honda, Y.; Kitao, O.; Nakai, H.; Vreven, T.; Montgomery, J. A., Jr.; Peralta, J. E.; Ogliaro, F.; Bearpark, M.; Heyd, J. J.; Brothers, E.; Kudin, K. N.; Staroverov, V. N.; Kobayashi, R.; Normand, J.; Raghavachari, K.; Rendell, A.; Burant, J. C.; Iyengar, S. S.; Tomasi, J.; Cossi, M.; Rega, N.; Millam, J. M.; Klene, M.; Knox, J. E.; Cross, J. B.; Bakken, V.; Adamo, C.; Jaramillo, J.; Gomperts, R.; Stratmann, R. E.; Yazyev, O.; Austin, A. J.; Cammi, R.; Pomelli, C.; Ochterski, J. W.; Martin, R. L.; Morokuma, K.; Zakrzewski, V. G.; Voth, G. A.; Salvador, P.; Dannenberg, J. J.; Dapprich, S.; Daniels, A. D.; Farkas, O.; Foresman, J. B.; Ortiz, J. V.; Cioslowski, J.; Fox, D. J.; *Gaussian09*, Rev. A.02; Gaussian, Inc.: Wallingford, CT, 2009.
(17) Both irreducibles, the non degenerated A and the doubly degenerated E, are both IR and Raman active (as can be seen in the character table in the Supporting Information) since the symmetry classes transform linearly and quadratically.
(18) Pyykkö, P.; Atsumi, M. *Chem.—Eur. J.* **2009**, *15*, 12770−12779.
(19) (a) Bondi, A. *J. Phys. Chem.* **1964**, *68*, 441−451. (b) Wiberg, H. *Lehrbuch der Anorganische Chemie*, 102. Auflage; Walter DeGruyter: Berlin, Germany, 2007; Anhang IV. (c) The value for r_{vdW}(Rh) was estimated 1.6, cf. r_{vdW}(Pd) = 1.63 Å.
(20) Schrock, R. R.; Osborn, J. A. *J. Am. Chem. Soc.* **1971**, *93*, 2397−2407.
(21) Sheldrick, G. M. *Acta Crystallogr., sect. A* **1997**, *64*, 112−122.
(22) *X-SHAPE, X-RED32 and X-AREA*; STOE & Cie: Darmstadt, Germany, 2005.